Check for updates

Geophysical Research Letters

RESEARCH LETTER
10.1029/2026GL123920

Interhemispheric Stratospheric Symmetry: Seasonal Precursors to Surface Extratropical Variability

Elizabeth Collingwood[1,2], **Adam A. Scaife**[3,4], **Gareth J. Marshall**[1], **and Bablu Sinha**[5]

[1]British Antarctic Survey, Cambridge, UK, [2]School of Ocean and Earth Science, University of Southampton, Southampton, UK, [3]Met Office Hadley Centre, Exeter, UK, [4]Department of Mathematics and Statistics, University of Exeter, Exeter, UK, [5]National Oceanography Centre, Southampton, UK

Key Points:

- Both hemispheres show analogous teleconnections between meridional wind in the upper stratosphere and the surface climate
- Upper stratospheric meridional wind in October is a skilful predictor of the surface Southern Annular Mode in austral summer
- Climate models are unable to reproduce these teleconnections likely because of misrepresentation of upper stratospheric dynamics

Supporting Information:

Supporting Information may be found in the online version of this article.

Correspondence to:

E. Collingwood,
e.collingwood@reading.ac.uk

Citation:

Collingwood, E., Scaife, A. A., Marshall, G. J., & Sinha, B. (2026). Interhemispheric stratospheric symmetry: Seasonal precursors to surface extratropical variability. *Geophysical Research Letters*, *53*, e2026GL123920. https://doi.org/10.1029/2026GL123920

Received 28 APR 2026
Accepted 13 OCT 2026

Abstract Seasonal prediction of surface climate relies on influences external to the troposphere, of which the stratosphere is a key source. The October stratosphere is particularly important for predictability of the coming winter and summer seasons in the Northern and Southern Hemisphere respectively, as the seasonal transition in zonal winds creates an interhemispherically symmetric window of stratosphere-troposphere coupling. Building on a recently identified teleconnection between the October upper stratospheric meridional wind and the December-January-February (DJF) North Atlantic Oscillation, we use reanalysis to demonstrate an analogous Southern Hemisphere teleconnection predicting the DJF Southern Annular Mode with skill ($r = 0.53$) comparable to current operational seasonal forecasts. We show that CMIP6 models fail to capture either teleconnection and that model skill is contingent on representation of the stratospheric pathway connecting the October meridional wind indices to the respective DJF polar vortex, a relationship that is poorly captured across models in both hemispheres.

Plain Language Summary Seasonal prediction (1–3 months ahead) of the surface climate is of societal importance as it allows for preparation and planning ahead of extreme weather and storminess. The stratosphere is a known source of seasonal predictability of the surface climate, particularly in winter for the Northern Hemisphere. In October, conditions in the stratosphere are undergoing seasonal transition in both hemispheres and are approximately symmetric during this month, suggesting that two parallel but independent pathways may connect October stratospheric conditions to the December-January-February climate in each hemisphere. This symmetry has not previously been investigated. Building on a study that identified the Northern Hemisphere pathway, we identify the Southern Hemisphere equivalent, which appears to be at least as strong. We also show that climate models fail to capture either pathway, likely because they poorly represent the stratospheric part of the connection.

1. Introduction

Seasonal prediction (1–3 months ahead) of surface climate remains a significant challenge in both hemispheres (Doblas-Reyes et al., 2013; Lim et al., 2013). Due to inherent internal variability, seasonal predictability relies on the existence of low frequency influences such as the stratosphere (Baldwin & Dunkerton, 2001; Domeisen et al., 2020; Kidston et al., 2015; Scaife et al., 2022), which projects onto the troposphere and surface via stratosphere-troposphere coupling (Kuroda & Kodera, 1998; Thompson & Wallace, 2000; Thompson et al., 2005). This coupling is particularly active during October through February in both hemispheres: in the Northern Hemisphere (NH) the zonal winds become westerly and accelerate into winter, while in the Southern Hemisphere (SH), with the transition to summer, the zonal winds are no longer prohibitively strong; in both cases this permits upward planetary wave propagation (Charney & Drazin, 1961; Kodera et al., 1990; Lim et al., 2018). The subsequent months see breakdowns in the stratospheric polar vortex, which create a path of downward coupling to the troposphere. This makes the period a unique window for stratospheric influence on surface climate via downward coupling that does not occur at other times of the year (Collingwood et al., 2024; Gray et al., 2022; Nie et al., 2019).

The North Atlantic Oscillation (NAO) is the leading mode of variability in the North Atlantic climate (Hurrell et al., 2001), whose seasonal prediction is of significant societal importance due to its intrinsic link to Euro-Atlantic weather and climate. While there is clear evidence of prediction skill for the surface NAO (Athanasiadis et al., 2017; Kang et al., 2014; Kent et al., 2022; Scaife et al., 2014a), success varies across different forecast

© 2026 The Author(s). Geophysical Research Letters published by Wiley Periodicals LLC on behalf of American Geophysical Union.
This is an open access article under the terms of the Creative Commons Attribution License, which permits use, distribution and reproduction in any medium, provided the original work is properly cited.

19448007, 2026, 20, Downloaded from https://agupubs.onlinelibrary.wiley.com/doi/10.1029/2026GL123920 by Catherine Beckett - University Of Southampton , Wiley Online Library on [12/11/2026]. See the Terms and Conditions (https://onlinelibrary.wiley.com/terms-and-conditions) on Wiley Online Library for rules of use; OA articles are governed by the applicable Creative Commons License

systems and climate models (Baker et al., 2018). A recent reanalysis study identified a significant source of seasonal December-January-February (DJF) NAO predictability in the October upper stratospheric meridional wind ($r = 0.38$) (Collingwood et al., 2024). The signal is primarily generated by anomalous eddy momentum flux divergence in the midlatitude upper stratosphere, which subsequently influences the wave breaking and absorption, and propagates a signal to the surface by established NH stratosphere-troposphere coupling pathways. Their study highlighted midlatitude meridional wind as a proxy for the Eulerian mean circulation response to early winter wave forcing and demonstrated its contribution to seasonal NAO predictability. Building on the interhemispheric symmetry in the stratospheric seasonal transition, we test whether an analogous teleconnection exists between the October stratospheric meridional winds and the summer (DJF) Southern Annular Mode (SAM).

The SAM is the leading mode of SH extratropical variability (Thompson & Wallace, 2000), influencing the Southern Ocean (Lovenduski & Gruber, 2005; Purich et al., 2025), regional temperature and rainfall (Fogt et al., 2012; Gillett et al., 2006; Hendon et al., 2007), Antarctic climate (Marshall et al., 2026), sea ice (Boehm et al., 2025), and extratropical circulation (Fogt & Marshall, 2020). Seasonal prediction of the SAM was believed difficult due to its relatively fast decorrelation time of ∼10 days (Robinson, 2000); however, some studies report significant skill for austral spring and early summer SAM (Lim et al., 2013; Seviour et al., 2014), with known sources of subseasonal-to-seasonal predictability including upper troposphere-lower stratosphere ozone (Zhu et al., 2025) and El Niño-Southern Oscillation (ENSO) (Fogt & Bromwich, 2006; Lim et al., 2013), providing limited and seasonally dependent skill. More recently, Byrne and Shepherd (2018) found significant seasonal predictability for summer polar vortex breakdown timing and the tropospheric circulation response (including the SAM) located in the middle stratosphere (Byrne et al., 2017), while Lim et al. (2018) similarly identified vortex breakdown and spring SAM predictability in the October middle stratosphere. This source of skill exists in the zonal wind and preconditions the stratosphere by modulating vertically propagating planetary wave activity and inducing a meridional shift of the vortex in the upper stratosphere. However, no study has utilized the interhemispheric symmetry of the October stratosphere-troposphere coupling window to examine whether analogous teleconnections like that of Collingwood et al. (2024) offer additional DJF SAM predictability.

Here we demonstrate an interhemispheric symmetry in the capacity of the October stratosphere to predict DJF surface climate, identifying a SH teleconnection between the October upper stratospheric meridional wind and DJF SAM. While the NH teleconnection focused on the regional NAO pattern, the present study focuses on the zonal SAM because the circulation in the SH is highly zonally symmetric and thus the stratospheric influence on the troposphere projects predominantly onto the annular mode. This symmetry illuminates both the shared dynamical mechanisms and the hemispheric differences in stratosphere-troposphere coupling pathways. We show that our SH October meridional wind index is linked to the timing of the SH polar vortex breakdown, providing a potential physical basis for the teleconnection consistent with Byrne and Shepherd (2018), while extending it to a specific upper stratospheric precursor not previously identified.

As model representation of stratospheric pathways is a known limiting factor in seasonal forecast skill (Domeisen et al., 2020; Garfinkel et al., 2017; Scaife et al., 2014), we investigate the representation of both teleconnections in 35 Coupled Model Intercomparison Project (CMIP6) models and a new climate model large ensemble. Current climate models exhibit considerable spread in their representations of the stratosphere (Hall et al., 2021; Karpechko et al., 2022) and provide ample data to study such teleconnections and identify sources of model error. Since operational forecasting systems share their underlying physics with the CMIP6 climate models but are also initialized from the observed state each forecast, a study using these climate models offers insight into whether the teleconnection exists as a feature of their own physics and internal variability, independent of any initialization. This aims to answer the question of whether seasonal forecasts are mechanistically able to recreate the teleconnections, without conducting the computationally expensive task of a direct skill assessment across operational forecast systems. We show that model teleconnection skill is contingent on accurate representation of the stratospheric connection between the October upper stratospheric meridional wind and the DJF polar vortices, a relationship that is poorly captured across models in both hemispheres.

2. Methodology

2.1. Data

This analysis uses ECMWF ERA5 reanalysis (Hersbach et al., 2020) sea level pressure (SLP), temperature, and zonal mean wind data for 1979–2025 (45 complete winters, 1979/80–2024/25); this longer period than

19448007, 2026, 20, Downloaded from https://agupubs.onlinelibrary.wiley.com/doi/10.1029/2026GL123920 by Catherine Beckett - University Of Southampton , Wiley Online Library on [12/11/2026]. See the Terms and Conditions (https://onlinelibrary.wiley.com/terms-and-conditions) on Wiley Online Library for rules of use; OA articles are governed by the applicable Creative Commons License

Collingwood et al. (2024) accounts for minor disparities between our reported values and theirs. 1979 marks the introduction of operational satellite sounder data and the consequent improvement in stratospheric accuracy, particularly in the SH (Marshall, 2002; Thompson & Solomon, 2002). ERA5 has a horizontal resolution of 0.25° and 137 levels to 80 km, including 60 levels between 0.01 and 100 hPa (Hersbach et al., 2023); we use 6-hourly data throughout. Pressure-level fields (temperature, zonal and meridional wind) are used at 0.5° resolution due to storage limitations, which is equivalent to taking every other point of the native 0.25° grid rather than area-averaged regridding.

Results were verified using MERRA-2 (Gelaro et al., 2017) (0.5° × 0.625°, 72 levels to 0.01 hPa, 1980-present) and JRA-55 (Harada et al., 2016; Kobayashi et al., 2015) (~0.56°, 60 levels to 0.1 hPa, 1958-present).

We analyze monthly output from historical simulations of 35 CMIP6 models (Eyring et al., 2016) (incomplete-data models excluded) over 1979–2014, the shared satellite-era period with reanalysis; native model grids are retained, but index regions/levels are interpolated to a common 1° grid for cross-model comparability. We also include the CANARI Large Ensemble (Schiemann et al., 2023) (1979–2014), using high-resolution HadGEM3-GC3.1 (N216, 60 km at midlatitudes, 40 members), whose size improves sampling of internal variability relative to individual CMIP6 models. Models and member counts are summarized in Table S1 of the Supporting Information S1. As 41% of all members use HadGEM3 physics, systematic HadGEM3 biases could be over-represented in the ensemble means; we do not correct for this but flag it as a limitation of unequal model representation.

2.2. Index Calculations

Collingwood et al. (2024) demonstrated that an index constructed using the meridional wind in the upper stratosphere is significantly linked to the subsequent winter NAO; the present study emulates this exact index and constructs an analogous index in the SH. The October v indices are the normalized zonally averaged meridional wind speed over the upper stratospheric surf zone (40°–60° latitude in the respective hemisphere, 1–3 hPa; mass-weighted), calculated in ERA5 using full resolution (0.25°) data for improved accuracy. The same calculation is applied to all the models but in their respective resolutions. This index region is sufficiently far poleward to evade the QBO-induced mean meridional circulation, which extends to 40° latitude in the upper stratosphere and significantly impacts the winter SPV in the NH (Holton & Tan, 1980) and, to a weaker extent, the SH (Baldwin & Dunkerton, 1998); correlations between the October QBO at 50 hPa and the October v indices are insignificant in both hemispheres (SH: $r = 0.12$, NH: $r = 0.19$).

We examine the ability of these indices to predict DJF surface SAM and NAO, calculated respectively as the zonally averaged SLP difference between 65° and 40°S (Gong & Wang, 1999), and the reanalysis SLP difference between the Azores (36°–40°N, 28°–20°W) and Iceland (63°–70°N, 25°–16°W) (Dunstone et al., 2016), although results remain significant for station- and principal component-based NAO indices too (NCAR, 2003). We also investigate the role of the stratospheric polar vortices, represented by the 10 hPa zonal-mean zonal wind at 60°S/N (the average latitude and height of strongest vortex winds). All indices are deseasonalized and detrended.

3. Results

3.1. Interhemispheric Symmetry

October represents a month of transition into a season of active stratosphere-troposphere coupling and vortex breakdowns (winter in NH, summer in SH), meaning its stratospheric conditions may inform DJF predictability. Figures 1a and 1b illustrates climatological October meridional and zonal wind respectively, from the surface to the upper stratosphere. It demonstrates that the strength, sign, and location of the Hadley and Ferrel cells, sub-tropical jets, and polar vortices are approximately symmetric across hemispheres. These are climatological conditions that modulate the vertical propagation of planetary Rossby waves (Kodera et al., 1990).

October also represents a key point of transition between different states, as shown in Figure 1c: the 10 hPa zonal winds at 60°S and 60°N, representing polar vortex strength, are relatively weak but still westerly. In the NH the polar vortex is forming in October and strengthens over the following 2 months, whereas the SH polar vortex is breaking down, remaining westerly until December. This transitional state exhibits substantial interannual variability, particularly in the SH (Figure 1d).

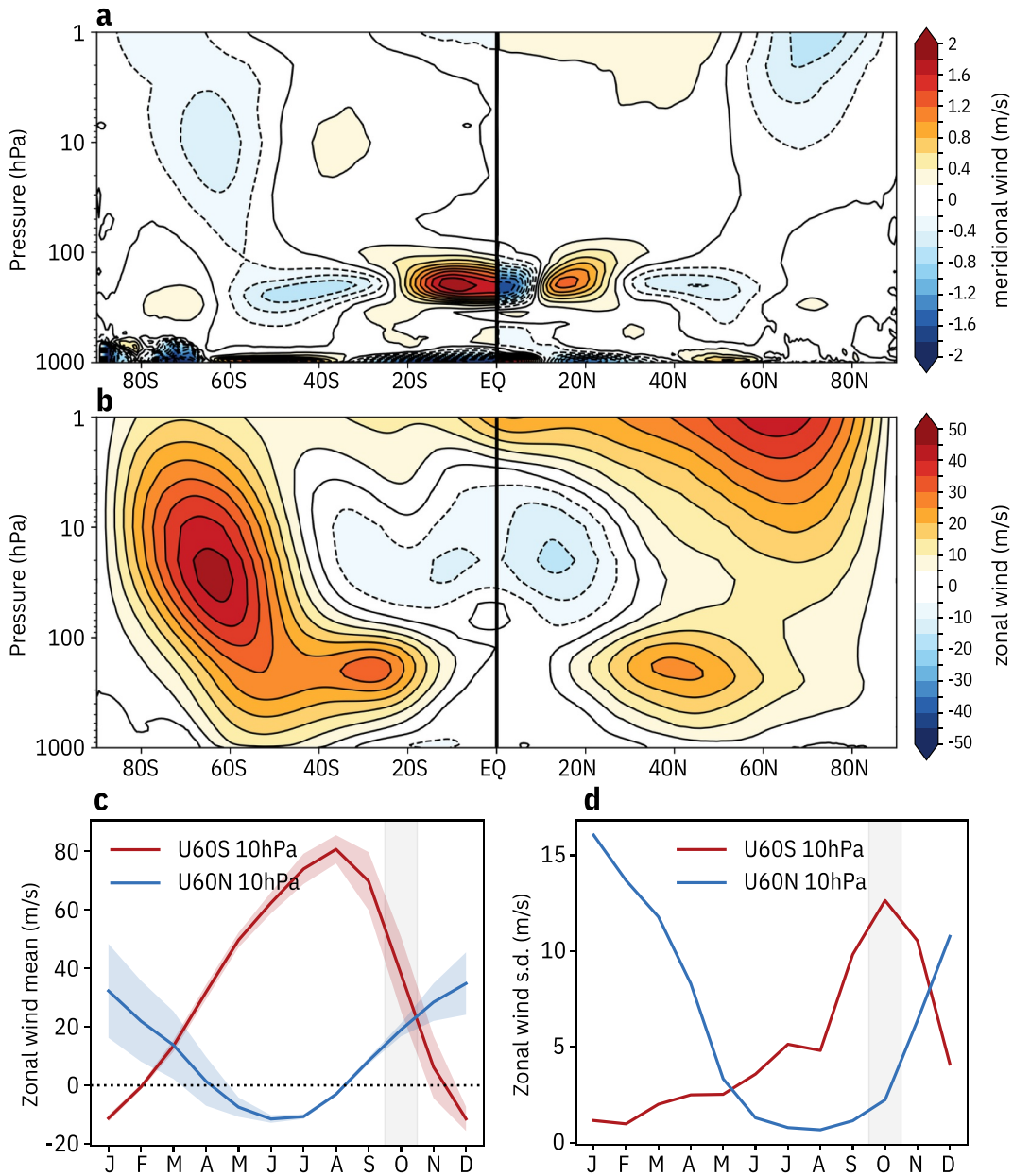


Figure 1. Interhemispheric symmetry in October climatology from ERA5 (1979–2025). (a) Meridional wind (positive = poleward) and (b) zonal wind climatologies. (c) Annual cycle of the mean and (d) annual cycle of the standard deviation, both for 10 hPa zonal wind at 60°S (red) and 60°N (blue), which is the approximate latitude and height of strongest vortex winds; envelopes in (c) denote interannual standard deviation. October is shaded gray.

This approximate symmetry (Figure 1a) includes a key source of DJF surface climate predictability. Collingwood et al. (2024) found the October upper stratosphere meridional wind to be a seasonal predictor of DJF NAO, and we use Figures 2a and 2b to show that the symmetric upper stratospheric midlatitude meridional wind (red box) supports DJF surface predictability in both hemispheres. In the SH, DJF SAM predictability is found in much of the mid-to-high latitude stratospheric meridional winds (Figure 2a), likely reflecting the concomitant strong zonal wind signal in Figure 2c. The signal appears slightly more poleward than in the NH (Figure 2b), though we continue to define OvSH using the red box for strict interhemispheric symmetry.

Figures 2c and 2d also reveals an apparent asymmetry: DJF SAM is strongly linked to October SH polar vortex strength, whereas the equivalent NH link is weak, but this reflects a hemispheric difference in coupling timing

19448007, 2026, 20, Downloaded from https://agupubs.onlinelibrary.wiley.com/doi/10.1029/2026GL123920 by Catherine Beckett - University Of Southampton , Wiley Online Library on [12/11/2026]. See the Terms and Conditions (https://onlinelibrary.wiley.com/terms-and-conditions) on Wiley Online Library for rules of use; OA articles are governed by the applicable Creative Commons License

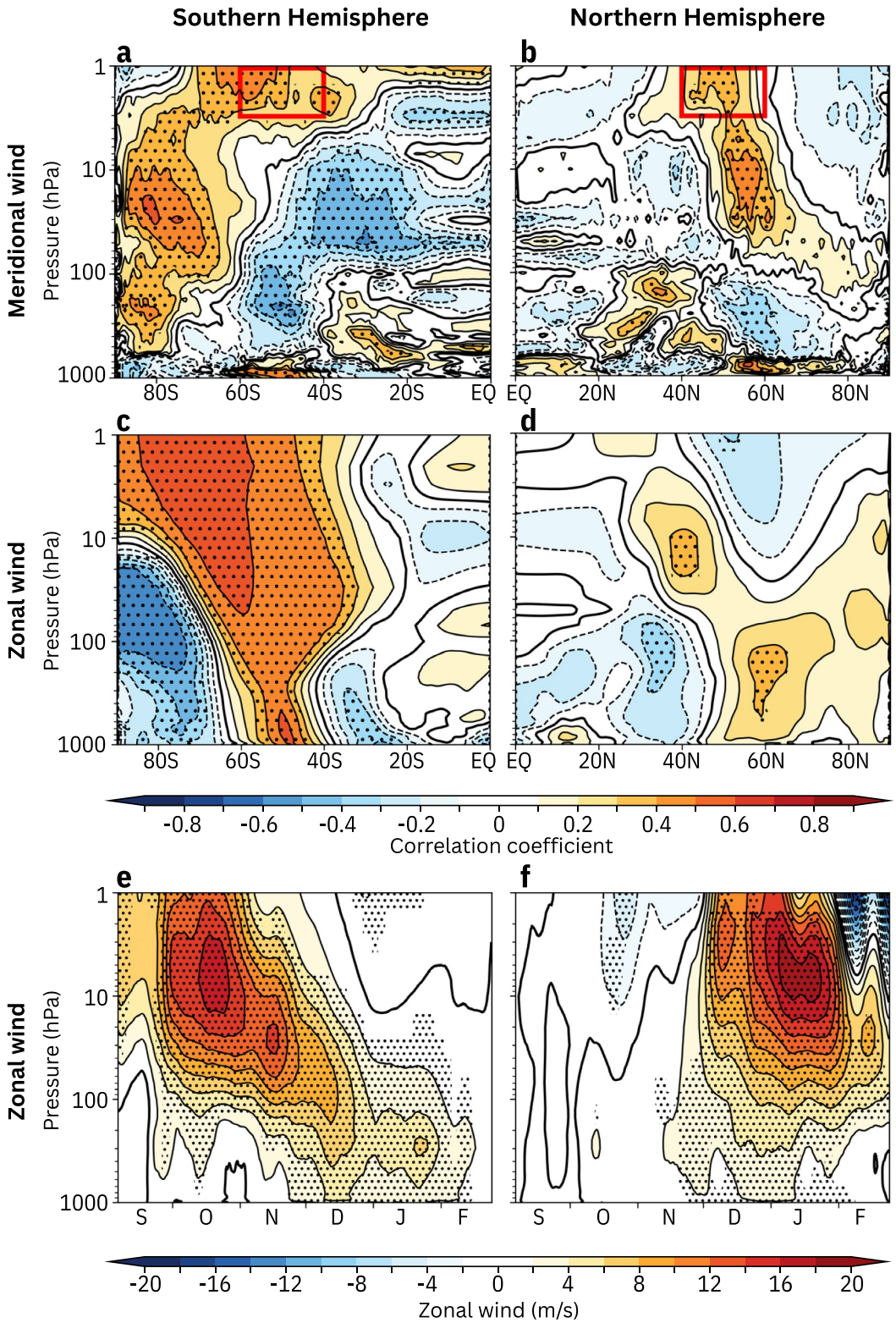


Figure 2. Relationship between the October atmosphere and DJF surface climate. Top row shows the correlation between the October meridional wind field and (a) DJF SAM and (b) DJF NAO. October v index regions are marked out by a red box. Second row shows the correlation between the October zonal wind field and (c) DJF SAM or (d) DJF NAO. Bottom row illustrates Hovmöller composite zonal wind anomalies over September-February for (e) 60°S zonal winds: positive minus negative DJF SAM years, and (f) 60°N zonal winds: positive minus negative DJF NAO years. Stippling denotes significance at 5% level using a Student's *t* test.

19448007, 2026, 20, Downloaded from https://agupubs.onlinelibrary.wiley.com/doi/10.1029/2026GL123920 by Catherine Beckett - University Of Southampton , Wiley Online Library on [12/11/2026]. See the Terms and Conditions (https://onlinelibrary.wiley.com/terms-and-conditions) on Wiley Online Library for rules of use; OA articles are governed by the applicable Creative Commons License

19448007, 2026, 20, Downloaded from https://agupubs.onlinelibrary.wiley.com/doi/10.1029/2026GL123920 by Catherine Beckett - University Of Southampton , Wiley Online Library on [12/11/2026]. See the Terms and Conditions (https://onlinelibrary.wiley.com/terms-and-conditions) on Wiley Online Library for rules of use; OA articles are governed by the applicable Creative Commons License

rather than a fundamental asymmetry. The Hovmöller diagrams in Figures 2e and 2f show that in the SH, downward propagation of stratospheric anomalies occurs in austral spring/early summer due to the final vortex breakdown (Byrne et al., 2017; Thompson et al., 2005), making October the key coupling window; in the NH, by contrast, coupling occurs later in boreal winter, linked to variability in winter vortex strength (Baldwin & Dunkerton, 2001; Matsuno, 1971; Shaw et al., 2010).

3.2. Teleconnection to DJF Surface Conditions

The October upper stratosphere has a known link to DJF NAO (Collingwood et al., 2024). Building on the symmetry established in Section 3.1, we test whether an analogous SH teleconnection exists, using the meridional wind over the regions denoted in Figures 2a and 2b to calculate the SH v index ("OvSH") and NH v index ("OvNH").

Figures 3a and 3b establishes that OvSH and DJF SAM have a correlation of $r = 0.53$ ($p < 0.001$), while OvNH and DJF NAO have a correlation of $r = 0.39$ ($p = 0.008$; the disparity against Collingwood et al. (2024) is due to the longer reanalysis record used here), corresponding to 27.9% and 15.3% of explained variance in DJF SAM and NAO, respectively. The "hit rate" (the percentage of winters in which the two indices have the same sign) of DJF NAO and OvNH both being anomalously positive or negative is 69.0%, compared to only 57.8% for DJF SAM and OvSH. The marker colors in Figures 3a and 3b indicate a relationship with the strength of the respective DJF polar vortices; OvNH is clearly linked to NH (major) SSW occurrence, as expected (Collingwood et al., 2024), but the single SH major SSW in 2002 is not associated with a remarkable OvSH or DJF SAM value. We note that the October indices from each hemisphere are largely independent (insignificant correlation, $r = 0.23$, $p = 0.123$).

Figures 3c and 3d displays the time series of these indices. The correlation between the SH indices is more temporally consistent, whereas the NH indices show an initially weak relationship until around 2005, followed by a strong relationship. This is possibly linked to multidecadal NAO variability, consistent with evidence that inter-model spread in multidecadal NAO variability depends strongly on stratosphere-troposphere coupling (Bonnet et al., 2024). A percentile bootstrap (1000 iterations, resampling years with replacement) confirms the greater temporal stability of the SH relationship, with a narrower 95% confidence interval ([0.29, 0.74] vs. [0.10, 0.66] for NH).

This and the previous section demonstrate interhemispheric stratospheric symmetry in October and the coupling window that follows, with both hemispheres supporting analogous teleconnections between the October upper stratosphere and DJF surface climate.

3.3. Model Evaluation

Here we investigate the CMIP6 models' representation of the October meridional wind teleconnections for both hemispheres (see Table S1 in Supporting Information S1 for model details). Figure 4 illustrates the distribution of the OvSH-SAM and OvNH-NAO teleconnections across all CMIP6 model members over the available period 1979/80–2013/14. The ERA5 teleconnection, for this same period, falls in the 99th percentile of the SH model distribution (Figure 4a), whose mean is significantly above zero, meaning the average sign is correctly captured but the magnitude generally too weak. ERA5 falls in the 98th percentile of the NH model teleconnection distribution (Figure 4b), which clusters around zero. These panels suggest that the teleconnections in both hemispheres are not adequately captured by current climate models.

Collingwood et al. (2024) found the stratospheric polar vortex to be a significant mediator of the NH teleconnection, so we might expect the same of the SH given the interhemispheric symmetry witnessed thus far. Figures 4c and 4d displays the average teleconnection across all CMIP6 members and the relationships between the DJF polar vortex and the October v and DJF surface indices, demonstrating that in both hemispheres the October v index-DJF polar vortex relationship is poorly captured (SH: $r = 0.08$; NH: $r < 0.01$). Meanwhile, models better capture the subsequent DJF vortex-to-surface pathway (SH: $r = 0.69$; NH: $r = 0.38$). This is too strong in the SH, possibly due to known over-representation of the modeled SAM decorrelation time or other SH circulation biases (Bracegirdle et al., 2020; Priestley et al., 2023). In summary, model representation of both teleconnections appears to break down at the initial connection from the October v index to the stratospheric polar vortex.

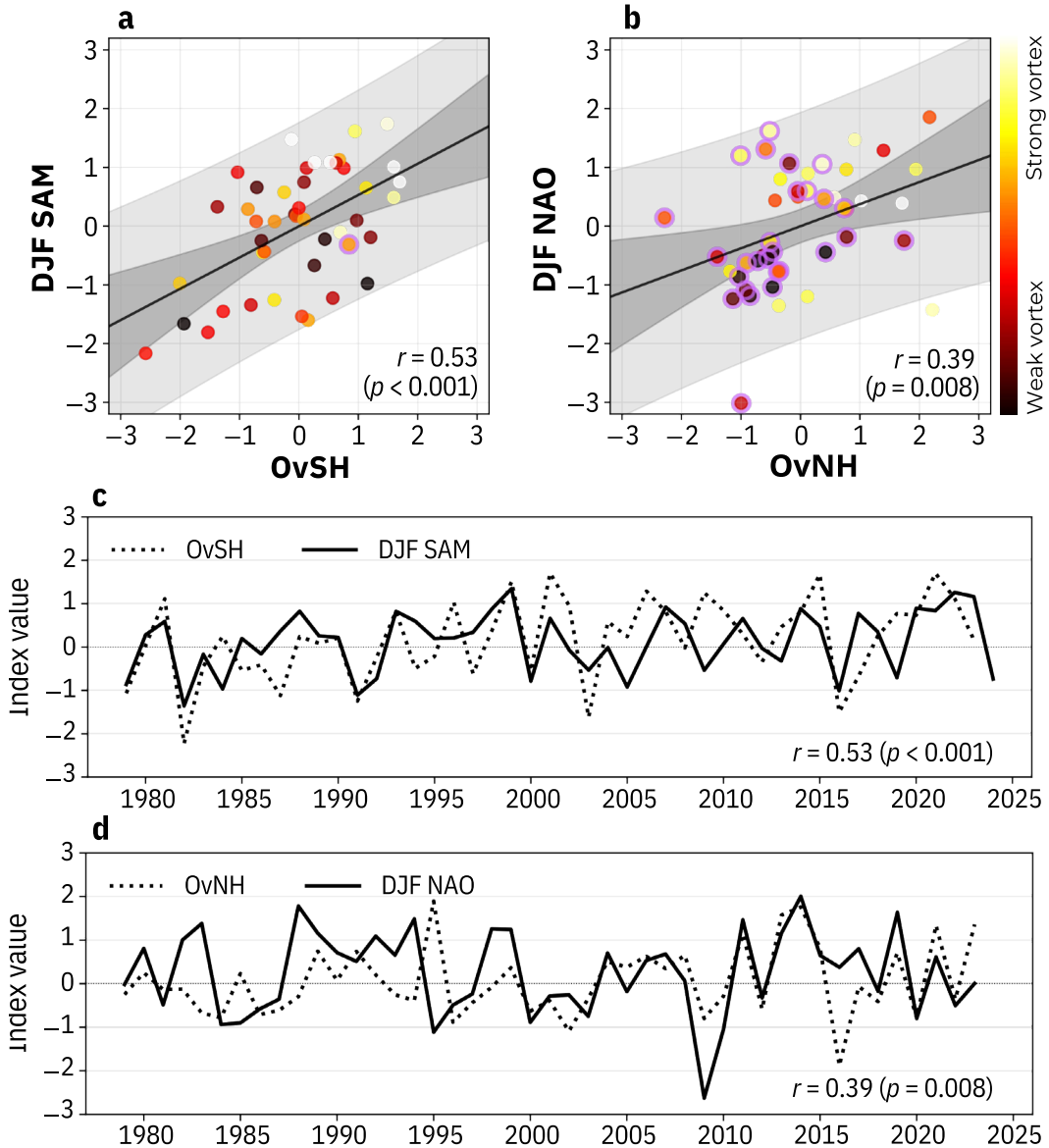


Figure 3. Interhemispheric symmetry in the teleconnections between October stratosphere and DJF surface climate. Scatterplots show (a) DJF SAM versus OvSH, and (b) DJF NAO versus OvNH. Marker colors indicate DJF stratospheric polar vortex strength. Purple circles denote SSW occurrence. Black line shows linear regression with 95% confidence intervals for the fitted line (dark gray) and prediction interval for individual predictions (light gray). Time series of (c) DJF SAM and OvSH, and (d) DJF NAO and OvNH.

Given this, how does the poor October v index–DJF polar vortex relationship impact overall modeled teleconnection error? Figures 5a and 5b shows that models with stronger October v index–DJF polar vortex relationships exhibit stronger October v index-DJF surface connections (SH: $r = 0.75, p < 0.001$; NH: $r = 0.43$, $p = 0.009$), whereas DJF polar vortex–surface coupling has no significant bearing on overall teleconnection skill (Figures 5c and 5d). This indicates that model representation of the full teleconnection in both hemispheres is conditional on the modeled strength of the October v index–DJF polar vortex relationship.

4. Discussion

In the SH, the climatological final warming is typically the only time of the year when the vortex breaks down, usually occurring in Nov-Dec. Meanwhile in the NH, the vortex has both the final warming in boreal spring, as

19448007, 2026, 20, Downloaded from https://agupubs.onlinelibrary.wiley.com/doi/10.1029/2026GL123920 by Catherine Beckett - University Of Southampton , Wiley Online Library on [12/11/2026]. See the Terms and Conditions (https://onlinelibrary.wiley.com/terms-and-conditions) on Wiley Online Library for rules of use; OA articles are governed by the applicable Creative Commons License

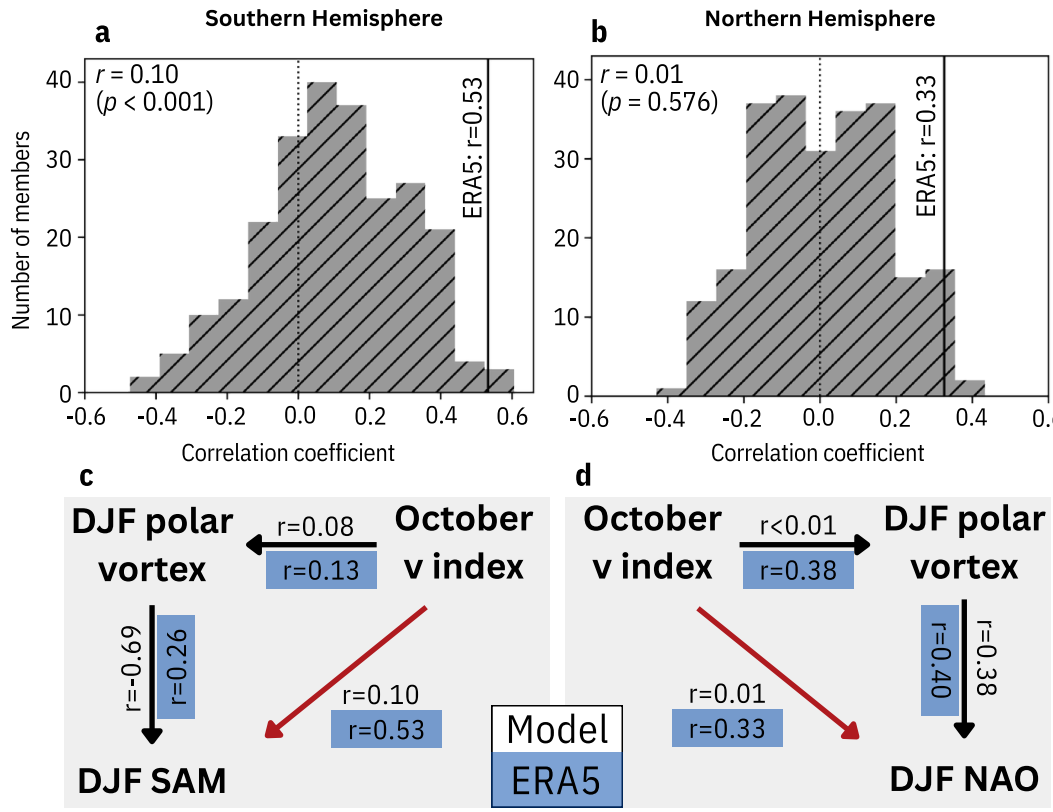


Figure 4. Models fail to capture either teleconnection or their stratospheric pathways. Distributions of individual member correlations in the available CMIP6 models for (a) the SH (OvSH-DJF SAM) teleconnection and (b) the NH (OvNH-DJF NAO) teleconnection. Corresponding ERA5 correlation coefficient for the shared period 1979–2014 is labeled. The schematics show the average member correlations and reanalysis correlations (in adjacent shaded boxes) representing the relationships between the October v indices, the DJF polar vortices, and DJF SAM/NAO, in (c) the SH and (d) the NH.

well as episodic weak vortex events occurring Nov-Mar. Despite these differences, both hemispheres offer analogous downward coupling pathways, with the longer SH timescale attributed to weaker wave forcing (Lim et al., 2018). Building on the NH teleconnection identified by Collingwood et al. (2024) (with $r = 0.39$), we have shown that an analogous relationship exists in the SH, whereby the October upper stratospheric meridional wind predicts DJF SAM with comparable skill ($r = 0.53$). We note that the NH teleconnection pertains to the NAO, not the northern annular mode (NAM), for which the teleconnection has a statistically insignificant coefficient of $r = 0.23$ ($p = 0.130$). This is consistent with Ambaum et al. (2001), who show that the NAO's link to the stratospheric polar vortex is well established and robust, while independent stratospheric forcing of the tropospheric NAM appears to be weaker. We further show that CMIP6 models generally fail to capture either teleconnection, and that for both hemispheres this failure is primarily attributed to poor representation of the stratospheric pathway connecting the October v indices to the respective DJF polar vortices.

The NH v wind-NAO teleconnection is significant at the 5% level in the reanalysis mean (ERA5, MERRA-2, JRA-55) over the shared period 1980–2012 ($r = 0.43$). The SH v wind-SAM correlation is also present in this ensemble ($r = 0.31$) but only significant at the 10% level, reflecting slight inter-reanalysis disagreement in the precise altitude of the predictability source, dampening the signal when averaged. This may relate to broader issues of fidelity in reanalysis representation of SH circulation (Marshall, 2003; Dell'Aquila et al., 2007). All three reanalyses nonetheless demonstrate significant DJF SAM predictability with comparable structure (not shown); we presented ERA5 here for its finer vertical resolution (Hersbach et al., 2020) and better representation of temporal continuity, circulation dynamics, and thermal structure (Essa et al., 2022; Kozubek et al., 2020; Orr et al., 2021).

19448007, 2026, 20, Downloaded from https://agupubs.onlinelibrary.wiley.com/doi/10.1029/2026GL123920 by Catherine Beckett - University Of Southampton , Wiley Online Library on [12/11/2026]. See the Terms and Conditions (https://onlinelibrary.wiley.com/terms-and-conditions) on Wiley Online Library for rules of use; OA articles are governed by the applicable Creative Commons License

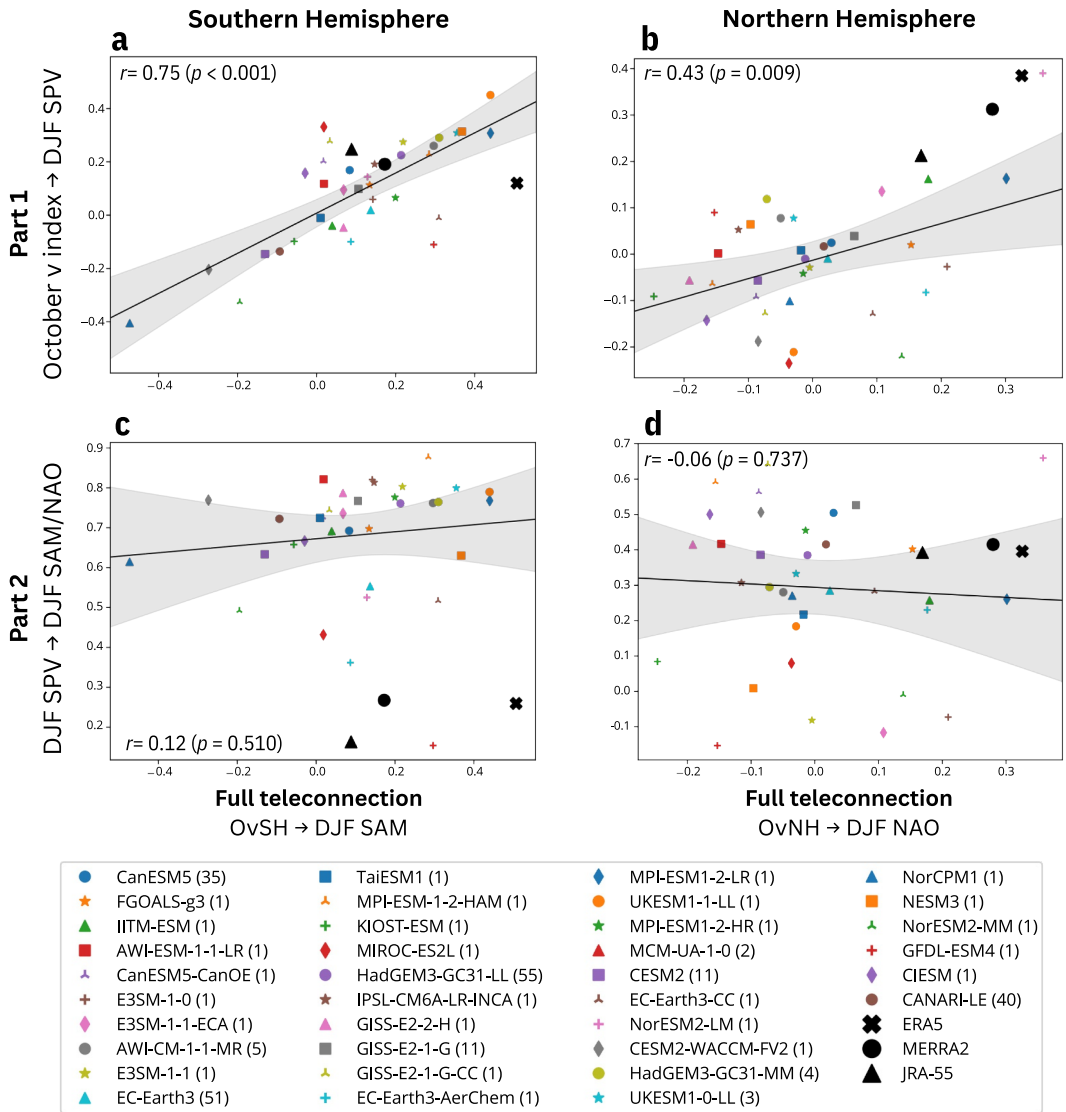


Figure 5. Model representation of the teleconnections depends on simulation of the stratospheric pathway. Scatter plots show the strength of each model's October v index–DJF surface teleconnection (*x*-axis) against the strength of mechanism components: October v index–DJF polar vortex relationship (a), (b); top, that is, Part 1) and DJF polar vortex–surface relationship (c), (d); bottom, that is, Part 2). (a), (c) SH (October SAM–DJF SAM). (b), (d) NH (October NAO–DJF NAO). Correlation coefficients and p values are shown. Number of members per model noted in key.

In the October NH, the meridional wind field is a better predictor of DJF NAO than the zonal wind field (Figures 2b and 2d). In the October SH, however, both fields are significantly correlated with DJF SAM, with Figure 2c illustrating a SAM signature in the October zonal winds. DJF SAM is significantly correlated with October SAM ($r = 0.36$, $p = 0.016$) and November SAM ($r = 0.44$, $p = 0.002$), reflecting known SAM persistence (Lorenz & Hartmann, 2001; Zhang et al., 2023) and raising the question of whether OvSH is simply passively responding to this persistence, rather than providing independent predictability. However, OvSH retains significant predictive skill for DJF SAM even when controlling for October SAM (partial $r = 0.51, p < 0.001$), demonstrating additional predictability beyond SAM autocorrelation alone. The October NAO-DJF NAO relationship, in contrast, shows no such persistence ($r = -0.06$), plausibly because NH downward coupling is associated with short, episodic SSW events, whereas SH coupling occurs through the climatological final warming, whose timing is shifted by preceding stratospheric conditions, producing an apparent persistence of the surface SAM (Byrne & Shepherd, 2018).

19448007, 2026, 20, Downloaded from https://agupubs.onlinelibrary.wiley.com/doi/10.1029/2026GL123920 by Catherine Beckett - University Of Southampton , Wiley Online Library on [12/11/2026]. See the Terms and Conditions (https://onlinelibrary.wiley.com/terms-and-conditions) on Wiley Online Library for rules of use; OA articles are governed by the applicable Creative Commons License

19448007, 2026, 20, Downloaded from https://agupubs.onlinelibrary.wiley.com/doi/10.1029/2026GL123920 by Catherine Beckett - University Of Southampton , Wiley Online Library on [12/11/2026]. See the Terms and Conditions (https://onlinelibrary.wiley.com/terms-and-conditions) on Wiley Online Library for rules of use; OA articles are governed by the applicable Creative Commons License

The seasonal predictability of DJF SAM using the October stratosphere is a new result, with skill ($r = 0.53$, $p < 0.001$) comparable to dynamical 1-month DJF SAM forecasts (Seviour et al., 2014). While statistically indistinguishable from the NH counterpart ($r = 0.39, p = 0.008$), the SH relationship exhibits smaller variability in its 10-year running mean, making it less susceptible to sampling variability that may undermine operational usefulness. Existing SAM seasonal predictability has been attributed primarily to ENSO (Lim et al., 2013), and the Pacific signal in the DJF SLP spatial correlation with OvSH (Figure S1a in Supporting Information S1) is consistent with the known positive SAM–La Niña association in austral summer (Clem & Fogt, 2013; Fogt & Bromwich, 2006; Fogt et al., 2011). However, this does not reflect ENSO having a role in the OvSH-DJF SAM relationship: controlling for October ENSO does not meaningfully alter the teleconnection ($r = 0.53$ to $r = 0.51$). It remains possible, though, that the ENSO signature reflects signal aliasing (shared covariability producing a spurious apparent relationship rather than a direct ENSO role) and separating these contributions warrants future investigation. We note that the statistical confidence of these results is constrained by the limited post-satellite era observational and model shared periods, particularly in the SH where sparse observational data limits verification.

Our study investigated CMIP6 model representation of both teleconnections, finding that in both hemispheres, skill is contingent on the relationship between the October v indices and the respective DJF polar vortices. Models poorly capture this relationship, perhaps unsurprising given well-documented CMIP6 biases in polar vortex strength and dynamics in both hemispheres (Bramberger & Bacmeister, 2025; Hall et al., 2021; Martínez-Andradas et al., 2025). To understand how model characteristics affect this, we split the mixed high-/low-top and -horizontal resolution CMIP6 models (Table S1 in Supporting Information S1 (Hall et al., 2021; Karpechko et al., 2022; Gerber & Manzini, 2016)); by resolution (threshold $\lesssim$100km, an approximately equal bisection) and model top (stratopause, $\sim$50km, as in Charlton-Perez et al. (2013)). For the OvSH-DJF SAM teleconnection (243 members), high-resolution members produce a stronger, more positive teleconnection than low-resolution members ($r = 0.13$ vs..0.06; $p = 0.004$, permutation test), as do high-top versus low-top members ($r = 0.12$ vs. -0.08; $p < 0.001$), with low-top/low-resolution members clustering around zero. The NH teleconnection, by contrast, is unanimously poorly captured across all subsamples.

CMIP6 teleconnection skill is unrelated to the DJF vortex-to-surface pathway, which is reasonably well captured (Figures 4c and 4d), suggesting the problem lies temporally or spatially upstream of the DJF polar vortex. This points to early winter stratospheric dynamics, rather than DJF vortex-troposphere coupling, as a more promising target for improving teleconnection fidelity in both hemispheres. The mechanism connecting the October v indices to the DJF polar vortex remains unclear, but we speculate that the anomalous meridional wind, or the wave forcing that generated it, modifies the potential vorticity gradient field and wave forcing in subsequent months, which impacts polar vortex development, and is consistent with prior literature on vortex preconditioning (Albers & Birner, 2014; Jucker & Reichler, 2018).

To assess OvSH's practical forecasting utility, we regressed DJF SAM onto OvSH and assessed skill via leave-one-out cross-validation to avoid overfitting. The cross-validated correlation ($r = 0.50$, $p < 0.001$) closely matches the in-sample value ($r = 0.53$), indicating a robust rather than overfitted relationship, and reduces the root mean square error (RMSE) by 13% relative to a climatological forecast. This demonstrates genuine additional skill for DJF SAM prediction, comparable to that reported for 1-month dynamical forecasts (Seviour et al., 2014).

Conflict of Interest

The authors declare no conflicts of interest relevant to this study.

Availability Statement

The ERA5 reanalysis hourly pressure level data (Hersbach et al., 2023) used in this study are freely available from https://doi.org/10.24381/cds.bd0915c6. The MERRA2 reanalysis data (Global Modeling and Assimilation Office (GMAO), 2015) are freely available from https://doi.org/10.5067/IUUF4WB9FT4W. The JRA-55 reanalysis data (Japan Meteorological Agency, 2013) are freely available from https://doi.org/10.5065/D60G3H5B. CMIP6 data are available from https://esgf-node.llnl.gov/projects/esgf-llnl/.

Acknowledgments
EC acknowledges support by the Natural Environment Research Council via the INSPIRE Doctoral Training Partnership. AAS was supported by the Met Office Hadley Centre Climate Programme (HCCP) funded by the UK Department for Science, Innovation and Technology (DSIT) and the UK Public Weather Service. GM and BS are supported by CANARI, a National Capability Multi-Centre Science programme of the Natural Environment Research Council (NEB2026, NE/W004984/1).

References

Albers, J. R., & Birner, T. (2014). Vortex preconditioning due to planetary and gravity waves prior to sudden stratospheric warmings. *Journal of the Atmospheric Sciences*, *71*(11), 4028–4054. https://doi.org/10.1175/JAS-D-14-0026.1

Ambaum, M. H., Hoskins, B. J., & Stephenson, D. B. (2001). Arctic oscillation or North Atlantic oscillation? *Journal of Climate*, *14*(16), 3495–3507. https://doi.org/10.1175/1520-0442(2001)014<3495:aoonao>2.0.co;2

Athanasiadis, P. J., Bellucci, A., Scaife, A. A., Hermanson, L., Materia, S., Sanna, A., et al. (2017). A multisystem view of wintertime NAO seasonal predictions. *Journal of Climate*, *30*(4), 1461–1475. https://doi.org/10.1175/JCLI-D-16-0153.1

Baker, L., Shaffrey, L., Sutton, R., Weisheimer, A., & Scaife, A. (2018). An intercomparison of skill and overconfidence/underconfidence of the wintertime North Atlantic Oscillation in multimodel seasonal forecasts. *Geophysical Research Letters*, *45*(15), 7808–7817. https://doi.org/10.1029/2018GL078838

Baldwin, M. P., & Dunkerton, T. J. (1998). Quasi-biennial modulation of the southern hemisphere stratospheric polar vortex. *Geophysical Research Letters*, *25*(17), 3343–3346. https://doi.org/10.1029/98gl02445

Baldwin, M. P., & Dunkerton, T. J. (2001). Stratospheric harbingers of anomalous weather regimes. *Science*, *294*(5542), 581–584. https://doi.org/10.1126/science.1063315

Boehm, C. L., Thompson, D. W., & Blanchard-Wrigglesworth, E. (2025). The key role of the southern annular mode during the sea-ice maximum for antarctic sea ice and its recent loss. *Communications Earth & Environment*, *6*(1), 833. https://doi.org/10.1038/s43247-025-02792-2

Bonnet, R., McKenna, C. M., & Maycock, A. C. (2024). Model spread in multidecadal North Atlantic oscillation variability connected to stratosphere–troposphere coupling. *Weather and Climate Dynamics*, *5*(3), 913–926. https://doi.org/10.5194/wcd-5-913-2024

Bracegirdle, T., Holmes, C., Hosking, J., Marshall, G., Osman, M., Patterson, M., & Rackow, T. (2020). Improvements in circumpolar Southern Hemisphere extratropical atmospheric circulation in CMIP6 compared to CMIP5. *Earth and Space Science*, *7*(6), e2019EA001065. https://doi.org/10.1029/2019ea001065

Bramberger, M., & Bacmeister, J. (2025). Improving representation of stratospheric polar vortex in Southern Hemisphere with low-frequency frontal waves. *Geophysical Research Letters*, *52*(20), e2025GL117854. https://doi.org/10.1029/2025gl117854

Byrne, N. J., & Shepherd, T. G. (2018). Seasonal persistence of circulation anomalies in the Southern Hemisphere stratosphere and its implications for the troposphere. *Journal of Climate*, *31*(9), 3467–3483. https://doi.org/10.1175/jcli-d-17-0557.1

Byrne, N. J., Shepherd, T. G., Woollings, T., & Plumb, R. A. (2017). Nonstationarity in Southern Hemisphere climate variability associated with the seasonal breakdown of the stratospheric polar vortex. *Journal of Climate*, *30*(18), 7125–7139. https://doi.org/10.1175/jcli-d-17-0097.1

Charlton-Perez, A. J., Baldwin, M. P., Birner, T., Black, R. X., Butler, A. H., Calvo Fernández, N., et al. (2013). On the lack of stratospheric dynamical variability in low-top versions of the CMIP5 models.

Charney, J. G., & Drazin, P. G. (1961). Propagation of planetary-scale disturbances from the lower into the upper atmosphere. *Journal of Geophysical Research (1896-1977)*, *66*(1), 83–109. https://doi.org/10.1029/JZ066i001p00083

Clem, K. R., & Fogt, R. L. (2013). Varying roles of ENSO and SAM on the Antarctic Peninsula climate in austral spring. *Journal of Geophysical Research: Atmospheres*, *118*(20), 11–481. https://doi.org/10.1002/jgrd.50860

Collingwood, E., Scaife, A. A., Lu, H., Sinha, B., King, J., Marsh, R., & Marshall, G. (2024). Meridional wind in the upper stratosphere: A source of winter NAO predictability. *Geophysical Research Letters*, *51*(24), e2024GL111717. https://doi.org/10.1029/2024gl111717

Dell'Aquila, A., Ruti, P. M., Calmanti, S., & Lucarini, V. (2007). Southern Hemisphere midlatitude atmospheric variability of the NCEP-NCAR and ECMWF reanalyses. *Journal of Geophysical Research*, *112*(D8). https://doi.org/10.1029/2006jd007376

Doblas-Reyes, F. J., García-Serrano, J., Lienert, F., Biescas, A. P., & Rodrigues, L. R. (2013). Seasonal climate predictability and forecasting: Status and prospects. *Wiley Interdisciplinary Reviews: Climate Change*, *4*(4), 245–268. https://doi.org/10.1002/wcc.217

Domeisen, D. I., Butler, A. H., Charlton-Perez, A. J., Ayarzagüena, B., Baldwin, M. P., Dunn-Sigouin, E., et al. (2020). The role of the stratosphere in subseasonal to seasonal prediction: 2. Predictability arising from stratosphere-troposphere coupling. *Journal of Geophysical Research: Atmospheres*, *125*(2), e2019JD030923. https://doi.org/10.1029/2019JD030923

Dunstone, N., Smith, D., Scaife, A., Hermanson, L., Eade, R., Robinson, N., et al. (2016). Skilful predictions of the winter North Atlantic Oscillation one year ahead. *Nature Geoscience*, *9*(11), 809–814. https://doi.org/10.1038/ngeo2824

Essa, Y. H., Cagnazzo, C., Madonna, F., Cristofanelli, P., Yang, C., Serva, F., et al. (2022). Intercomparison of atmospheric upper-air temperature from recent global reanalysis datasets. *Frontiers in Earth Science*, *10*, 935139. https://doi.org/10.3389/feart.2022.935139

Eyring, V., Bony, S., Meehl, G. A., Senior, C. A., Stevens, B., Stouffer, R. J., & Taylor, K. E. (2016). Overview of the coupled model intercomparison project phase 6 (CMIP6) experimental design and organization. *Geoscientific Model Development*, *9*(5), 1937–1958. https://doi.org/10.5194/gmd-9-1937-2016

Fogt, R. L., & Bromwich, D. H. (2006). Decadal variability of the ENSO teleconnection to the high-latitude south Pacific governed by coupling with the southern annular mode. *Journal of Climate*, *19*(6), 979–997. https://doi.org/10.1175/jcli3671.1

Fogt, R. L., Bromwich, D. H., & Hines, K. M. (2011). Understanding the sam influence on the South Pacific ENSO teleconnection. *Climate Dynamics*, *36*(7), 1555–1576. https://doi.org/10.1007/s00382-010-0905-0

Fogt, R. L., Jones, J. M., & Renwick, J. (2012). Seasonal zonal asymmetries in the southern annular mode and their impact on regional temperature anomalies. *Journal of Climate*, *25*(18), 6253–6270. https://doi.org/10.1175/jcli-d-11-00474.1

Fogt, R. L., & Marshall, G. J. (2020). The southern annular mode: Variability, trends, and climate impacts across the Southern Hemisphere. *Wiley Interdisciplinary Reviews: Climate Change*, *11*(4), e652. https://doi.org/10.1002/wcc.652

Garfinkel, C. I., Son, S.-W., Song, K., Aquila, V., & Oman, L. D. (2017). Stratospheric variability contributed to and sustained the recent hiatus in Eurasian winter warming. *Geophysical Research Letters*, *44*(1), 374–382. https://doi.org/10.1002/2016gl072035

Gelaro, R., McCarty, W., Suárez, M. J., Todling, R., Molod, A., Takacs, L., et al. (2017). The modern-era retrospective analysis for research and applications, version 2 (MERRA-2). *Journal of Climate*, *30*(14), 5419–5454. https://doi.org/10.1175/JCLI-D-16-0758.1

Gerber, E. P., & Manzini, E. (2016). The dynamics and variability model intercomparison project (dynvarmip) for CMIP6: Assessing the stratosphere–troposphere system. *Geoscientific Model Development*, *9*(9), 3413–3425. https://doi.org/10.5194/gmd-9-3413-2016

Gillett, N. P., Kell, T. D., & Jones, P. (2006). Regional climate impacts of the southern annular mode. *Geophysical Research Letters*, *33*(23). https://doi.org/10.1029/2006gl027721

Global Modeling and Assimilation Office (GMAO). (2015). MERRA-2 inst6_3d_ana_nv: 3d, 6-hourly, instantaneous, model-level, analysis, analyzed meteorological fields v5.12.4 [Dataset]. *Goddard Earth Sciences Data and Information Services Center (GES DISC)*. https://doi.org/10.5067/IUUF4WB9FT4W

Gong, D., & Wang, S. (1999). Definition of antarctic oscillation index. *Geophysical Research Letters*, *26*(4), 459–462. https://doi.org/10.1029/1999gl900003

19448007, 2026, 20, Downloaded from https://agupubs.onlinelibrary.wiley.com/doi/10.1029/2026GL123920 by Catherine Beckett - University Of Southampton , Wiley Online Library on [12/11/2026]. See the Terms and Conditions (https://onlinelibrary.wiley.com/terms-and-conditions) on Wiley Online Library for rules of use; OA articles are governed by the applicable Creative Commons License

Gray, L. J., Lu, H., Brown, M. J., Knight, J. R., & Andrews, M. B. (2022). Mechanisms of influence of the semi-annual oscillation on stratospheric sudden warmings. *Quarterly Journal of the Royal Meteorological Society*, *148*(744), 1223–1241. https://doi.org/10.1002/qj.4256

Hall, R. J., Mitchell, D. M., Seviour, W. J., & Wright, C. J. (2021). Persistent model biases in the CMIP6 representation of stratospheric polar vortex variability. *Journal of Geophysical Research: Atmospheres*, *126*(12), e2021JD034759. https://doi.org/10.1029/2021jd034759

Harada, Y., Kamahori, H., Kobayashi, C., Endo, H., Kobayashi, S., Ota, Y., et al. (2016). The jra-55 reanalysis: Representation of atmospheric circulation and climate variability. *Journal of the Meteorological Society of Japan. Series II*, *94*(3), 269–302. https://doi.org/10.2151/jmsj.2016-015

Hendon, H. H., Thompson, D. W., & Wheeler, M. C. (2007). Australian rainfall and surface temperature variations associated with the Southern Hemisphere annular mode. *Journal of Climate*, *20*(11), 2452–2467. https://doi.org/10.1175/jcli4134.1

Hersbach, H., Bell, B., Berrisford, P., Biavati, G., Horányi, A., Muñoz Sabater, J., et al. (2023). ERA5 hourly data on pressure levels from 1940 to present [Dataset]. *Copernicus Climate Change Service (C3S) Climate Data Store (CDS)*. https://doi.org/10.24381/cds.bd0915c6

Hersbach, H., Bell, B., Berrisford, P., Hirahara, S., Horányi, A., Muñoz-Sabater, J., et al. (2020). The ERA5 global reanalysis. *Quarterly Journal of the Royal Meteorological Society*, *146*(730), 1999–2049. https://doi.org/10.1002/qj.3803

Holton, J. R., & Tan, H.-C. (1980). The influence of the equatorial quasi-biennial oscillation on the global circulation at 50 mb. *Journal of the Atmospheric Sciences*, *37*(10), 2200–2208. https://doi.org/10.1175/1520-0469(1980)037<2200:tioteq>2.0.co;2

Hurrell, J. W., Kushnir, Y., & Visbeck, M. (2001). The North Atlantic Oscillation. *Science*, *291*(5504), 603–605. https://doi.org/10.1126/science.1058761

Japan Meteorological Agency. (2013). Japanese 55-year reanalysis, monthly means and variances (updated irregularly) [Dataset]. *NSF National Center for Atmospheric Research*. https://doi.org/10.5065/D60G3H5B

Jucker, M., & Reichler, T. (2018). Dynamical precursors for statistical prediction of stratospheric sudden warming events. *Geophysical Research Letters*, *45*(23), 13–124. https://doi.org/10.1029/2018gl080691

Kang, D., Lee, M.-I., Im, J., Kim, D., Kim, H.-M., Kang, H.-S., et al. (2014). Prediction of the Arctic Oscillation in boreal winter by dynamical seasonal forecasting systems. *Geophysical Research Letters*, *41*(10), 3577–3585. https://doi.org/10.1002/2014gl060011

Karpechko, A. Y., Afargan-Gerstman, H., Butler, A. H., Domeisen, D. I., Kretschmer, M., Lawrence, Z., et al. (2022). Northern hemisphere stratosphere-troposphere circulation change in CMIP6 models: 1. Inter-model spread and scenario sensitivity. *Journal of Geophysical Research: Atmospheres*, *127*(18), e2022JD036992. https://doi.org/10.1029/2022jd036992

Kent, C., Scaife, A. A., & Dunstone, N. (2022). What potential for improving sub-seasonal predictions of the winter NAO. *Atmospheric Science Letters*, *24*(4), e1146. https://doi.org/10.1002/asl.1146

Kidston, J., Scaife, A. A., Hardiman, S. C., Mitchell, D. M., Butchart, N., Baldwin, M. P., & Gray, L. J. (2015). Stratospheric influence on tropospheric jet streams, storm tracks and surface weather. *Nature Geoscience*, *8*(6), 433–440. https://doi.org/10.1038/ngeo2424

Kobayashi, S., Ota, Y., Harada, Y., Ebita, A., Moriya, M., Onoda, H., et al. (2015). The JRA-55 reanalysis: General specifications and basic characteristics. *Journal of the Meteorological Society of Japan. Series II*, *93*(1), 5–48. https://doi.org/10.2151/jmsj.2015-001

Kodera, K., Yamazaki, K., Chiba, M., & Shibata, K. (1990). Downward propagation of upper stratospheric mean zonal wind perturbation to the troposphere. *Geophysical Research Letters*, *17*(9), 1263–1266. https://doi.org/10.1029/GL017i009p01263

Kozubek, M., Krizan, P., & Lastovicka, J. (2020). Homogeneity of the temperature data series from ERA5 and MERRA2 and temperature trends. *Atmosphere*, *11*(3), 235. https://doi.org/10.3390/atmos11030235

Kuroda, Y., & Kodera, K. (1998). Interannual variability in the troposphere and stratosphere of the Southern Hemisphere winter. *Journal of Geophysical Research*, *103*(D12), 13787–13799. https://doi.org/10.1029/98jd01042

Lim, E.-P., Hendon, H. H., & Rashid, H. (2013). Seasonal predictability of the southern annular mode due to its association with enso. *Journal of Climate*, *26*(20), 8037–8054. https://doi.org/10.1175/jcli-d-13-00006.1

Lim, E.-P., Hendon, H. H., & Thompson, D. W. (2018). Seasonal evolution of stratosphere-troposphere coupling in the Southern Hemisphere and implications for the predictability of surface climate. *Journal of Geophysical Research: Atmospheres*, *123*(21), 12002–12016. https://doi.org/10.1029/2018jd029321

Lorenz, D. J., & Hartmann, D. L. (2001). Eddy–zonal flow feedback in the Southern Hemisphere. *Journal of the Atmospheric Sciences*, *58*(21), 3312–3327. https://doi.org/10.1175/1520-0469(2001)058<3312:ezffit>2.0.co;2

Lovenduski, N. S., & Gruber, N. (2005). Impact of the southern annular mode on Southern Ocean circulation and biology. *Geophysical Research Letters*, *32*(11). https://doi.org/10.1029/2005gl022727

Marshall, G. J., Williams, R. S., Graff, L. S., Handorf, D., Karpechko, A. Y., Köhler, R. H., et al. (2026). The southern annular mode and its relationship with Antarctic temperature in contrasting future storylines. *Climate Dynamics*, *64*(2), 79. https://doi.org/10.1007/s00382-026-08081-8

Marshall, G. J. (2002). Trends in Antarctic geopotential height and temperature: A comparison between radiosonde and NCEP–NCAR reanalysis data. *Journal of Climate*, *15*(6), 659–674. https://doi.org/10.1175/1520-0442(2002)015<0659:tiagha>2.0.co;2

Marshall, G. J. (2003). Trends in the southern annular mode from observations and reanalyses. *Journal of Climate*, *16*(24), 4134–4143. https://doi.org/10.1175/1520-0442(2003)016<4134:titsam>2.0.co;2

Martínez-Andradas, V., de la Cámara, A., Zurita-Gotor, P., Lott, F., & Serva, F. (2025). Quantifying the spread in sudden stratospheric warming wave forcing in CMIP6. *Weather and Climate Dynamics*, *6*(1), 329–343. https://doi.org/10.5194/wcd-6-329-2025

Matsuno, T. (1971). A dynamical model of the stratospheric sudden warming. *Journal of the Atmospheric Sciences*, *28*(8), 1479–1494. https://doi.org/10.1175/1520-0469(1971)028⟨1479:ADMOTS⟩2.0.CO;2

NCAR, U. J. H. (2003). NAO index data provided by the climate analysis section. Retrieved from https://climatedataguide.ucar.edu/climate-data

Nie, Y., Scaife, A. A., Ren, H.-L., Comer, R. E., Andrews, M. B., Davis, P., & Martin, N. (2019). Stratospheric initial conditions provide seasonal predictability of the North Atlantic and Arctic Oscillations. *Environmental Research Letters*, *14*(3), 034006. https://doi.org/10.1088/1748-9326/ab0385

Orr, A., Lu, H., Martineau, P., Gerber, E. P., Marshall, G. J., & Bracegirdle, T. J. (2021). Is our dynamical understanding of the circulation changes associated with the antarctic ozone hole sensitive to the choice of reanalysis dataset? *Atmospheric Chemistry and Physics*, *21*(10), 7451–7472. https://doi.org/10.5194/acp-21-7451-2021

Priestley, M. D., Ackerley, D., Catto, J. L., & Hodges, K. I. (2023). Drivers of biases in the CMIP6 extratropical storm tracks. Part II: Southern Hemisphere. *Journal of Climate*, *36*(5), 1469–1486. https://doi.org/10.1175/jcli-d-20-0977.1

Purich, A., Arblaster, J. M., Boschat, G., Gillett, Z. E., Hobbs, W., Jucker, M., et al. (2025). Southern annular mode dynamics, projections and impacts in a changing climate. *Nature Reviews Earth & Environment*, 1–19.

Robinson, W. A. (2000). A baroclinic mechanism for the eddy feedback on the zonal index. *Journal of the Atmospheric Sciences*, *57*(3), 415–422. https://doi.org/10.1175/1520-0469(2000)057⟨0415:ABMFTE⟩2.0.CO;2

19448007, 2026, 20, Downloaded from https://agupubs.onlinelibrary.wiley.com/doi/10.1029/2026GL123920 by Catherine Beckett - University Of Southampton , Wiley Online Library on [12/11/2026]. See the Terms and Conditions (https://onlinelibrary.wiley.com/terms-and-conditions) on Wiley Online Library for rules of use; OA articles are governed by the applicable Creative Commons License

Scaife, A. A., Arribas, A., Blockley, E., Brookshaw, A., Clark, R., Dunstone, N., et al. (2014). Skillful long-range prediction of European and North American winters. *Geophysical Research Letters*, *41*(7), 2514–2519. https://doi.org/10.1002/2014GL059637

Scaife, A. A., Athanassiadou, M., Andrews, M., Arribas, A., Baldwin, M., Dunstone, N., et al. (2014). Predictability of the quasi-biennial oscillation and its northern winter teleconnection on seasonal to decadal timescales. *Geophysical Research Letters*, *41*(5), 1752–1758. https://doi.org/10.1002/2013gl059160

Scaife, A. A., Baldwin, M. P., Butler, A. H., Charlton-Perez, A. J., Domeisen, D. I., Garfinkel, C. I., et al. (2022). Long-range prediction and the stratosphere. *Atmospheric Chemistry and Physics*, *22*(4), 2601–2623. https://doi.org/10.5194/acp-22-2601-2022

Schiemann, R., Shaffrey, L., Lister, G., Hatcher, R., Wilson, S., Lawrence, B., et al. (2023). The CANARI science programme and HadGEM3 large ensemble. In *Xxviii general assembly of the international union of geodesy and geophysics (IUGG)*.

Seviour, W. J., Hardiman, S. C., Gray, L. J., Butchart, N., MacLachlan, C., & Scaife, A. A. (2014). Skillful seasonal prediction of the southern annular mode and Antarctic ozone. *Journal of Climate*, *27*(19), 7462–7474. https://doi.org/10.1175/jcli-d-14-00264.1

Shaw, T. A., Perlwitz, J., & Harnik, N. (2010). Downward wave coupling between the stratosphere and troposphere: The importance of meridional wave guiding and comparison with zonal-mean coupling. *Journal of Climate*, *23*(23), 6365–6381. https://doi.org/10.1175/2010JCLI3804.1

Thompson, D. W., Baldwin, M. P., & Solomon, S. (2005). Stratosphere–troposphere coupling in the Southern Hemisphere. *Journal of the Atmospheric Sciences*, *62*(3), 708–715. https://doi.org/10.1175/jas-3321.1

Thompson, D. W., & Solomon, S. (2002). Interpretation of recent Southern Hemisphere climate change. *Science*, *296*(5569), 895–899. https://doi.org/10.1126/science.1069270

Thompson, D. W., & Wallace, J. M. (2000). Annular modes in the extratropical circulation. Part I: Month-to-month variability. *Journal of Climate*, *13*(5), 1000–1016. https://doi.org/10.1175/1520-0442(2000)013<1000:amitec>2.0.co;2

Zhang, Q., Zhang, Y., & Wu, Z. (2023). Multiple time scales of the southern annular mode. *Climate Dynamics*, *61*(1), 1–18. https://doi.org/10.1007/s00382-022-06476-x

Zhu, L., Wu, Z., & Wang, B. (2025). Role of Antarctic ozone in shaping East Asian summer precipitation variability. *npj Climate and Atmospheric Science*, *8*(1), 234. https://doi.org/10.1038/s41612-025-01116-7

19448007, 2026, 20, Downloaded from https://agupubs.onlinelibrary.wiley.com/doi/10.1029/2026GL123920 by Catherine Beckett - University Of Southampton , Wiley Online Library on [12/11/2026]. See the Terms and Conditions (https://onlinelibrary.wiley.com/terms-and-conditions) on Wiley Online Library for rules of use; OA articles are governed by the applicable Creative Commons License